DMRG and Exact Diagonalization Applications of Bose-Hubbard Type Models

July 4, 2014

Contents

0.1 Tight Binding Model

Tight binding Hamiltonian in the second quantized form is

$$H = -J \sum_{j=0}^{M-1} (a_j^\dagger a_{j+1} + a_j a_{j+1}^\dagger) \tag{1}$$

in which $a_i^\dagger, a_{j+1}^\dagger$ are the bosonic creation operators on sites at $x_j = ja$ and $x_{j+1} = (j+1)a$ and a_j, a_{j+1} are the bosonic annihilation operators on sites x_j and x_{j+1} where a is the lattice parameter. Let $|j\rangle$ denote the state with one photon at site j, i.e.

$$\begin{aligned}
|1\rangle &= |n_0 n_1 \cdots n_{j-1} n_j n_{j+1} \cdots n_{M-2} n_{M-1}\rangle \\
&= |10\cdots000\cdots00\rangle \\
|2\rangle &= |01\cdots000\cdots00\rangle \\
&\vdots \quad \vdots \\
|j\rangle &= |00\cdots010\cdots00\rangle \\
&\vdots \quad \vdots \\
|M-1\rangle &= |00\cdots000\cdots01\rangle
\end{aligned}$$

and $|k\rangle$ the Fourier transform as below

$$|k\rangle = \frac{1}{\sqrt{M}} \sum_{j=0}^{M-1} e^{ikx_j} |j\rangle \tag{2}$$

with the periodic boundry conditions $x_{N+1} = x_1$.

We calculate the expectation value of the Hamiltonian by using the Eq 2.

$$H\left|k\right\rangle = \frac{1}{\sqrt{M}}\sum_{j=0}^{M-1} e^{ikx_j} H\left|j\right\rangle \tag{3}$$

By multiplying Eq 3 from left by $\left|k'\right\rangle$

$$\left\langle k'\right| H\left|k\right\rangle = \frac{1}{M}\sum_{j,j'} e^{i(kj-k'j')a}\left\langle j'\right| H\left|j\right\rangle \tag{4}$$

Considering the operation of Eq 3, Eq 4 has nonzero elements only for $j' = j \pm 1$ cases.

Then, Eq 4 becomes

$$\epsilon_k = \frac{1}{M}\sum_{j=0}^{M-1}\left(e^{ik'a}e^{ija(k-k')}\left\langle j-1\right| H\left|j\right\rangle + e^{-ik'a}e^{ija(k-k')}\left\langle j+1\right| H\left|j\right\rangle\right) \tag{5}$$

where $\sum_{j=0}^{M-1} e^{ija(k-k')} = M\delta_{kk'}$. Off diagonal elements of the Hamiltonian are some multiples of the hopping constant $-J$ in Eq 1.

$$\left\langle j-1\right| H\left|j\right\rangle = \left\langle j+1\right| H\left|j\right\rangle = 1 \tag{6}$$

Replacing Eq 6 in Eq 5 ϵ_k is founded as

$$\epsilon_k = -2J\cos(ka) \tag{7}$$

in which $ka = n\pi$, $n = 0, \pm 1, \cdots$ integer values. Since energy ϵ_k is a periodic function, all the energy values are obtained between $k = -\frac{\pi}{a}, \frac{\pi}{a}$ corresponding to the 1^{st} Brillouin zone.

Another way of finding the dispersion relation Eq 7 is showing $\left|k\right\rangle$ momentum states are the eigenstates of the Hamiltonian Eq 1 in the presence of periodic boundry conditions.

$$\begin{aligned}
H\left|k\right\rangle &= \epsilon_k\left|k\right\rangle && (8)\\
&= \frac{1}{\sqrt{M}}\sum_{j=0}^{M-1} e^{ikx_j} H\left|j\right\rangle && (9)\\
&= \frac{1}{\sqrt{M}}\sum_{j=0}^{M-1} e^{ikx_j}(\left|j+1\right\rangle + \left|j-1\right\rangle) && (10)\\
&= \frac{1}{\sqrt{M}}\sum_{j=0}^{M-1}(e^{ika(j+1)-ika)}\left|j+1\right\rangle + e^{ika(j-1)+ika)}\left|j-1\right\rangle) && (11)
\end{aligned}$$

by using the definition of $x_j = ja$. Periodic boundry conditions allows the states be $|0\rangle = |M\rangle$ and $|M-1\rangle = ket{-}1$. Hence, we can expand the Eq 11 as

$$\sum_{j=0}^{M-1} e^{ika(j+1)} |j+1\rangle = e^{-ika}\left(e^{ika}|1\rangle + e^{2ika}|2\rangle + e^{3ika}|3\rangle + \cdots + |0\rangle\right) \tag{12}$$

$$\sum_{j=0}^{M-1} e^{ika(j-1)} |j-1\rangle = \left(e^{ika(M-1)}|M-1\rangle + e^{ikMa}|M\rangle + e^{ika}|1\rangle + \cdots + e^{ika(M-2)}|M-2\rangle\right) \tag{13}$$

which are both equal to $\sum_{j=0}^{M-1} e^{ikja}|j\rangle$. Accoridngly, Eq 11 becomes

$$-2J\cos(ka)\frac{1}{\sqrt{(M)}}\sum_{j=0}^{M-1} e^{ikja}|j\rangle = \epsilon_k \frac{1}{\sqrt{(M)}}\sum_{j=0}^{M-1} e^{ikja}|j\rangle \tag{14}$$

where $\epsilon_k = -2J\cos(ka)$ is the dispersion relation which we obtained in Eq 4.

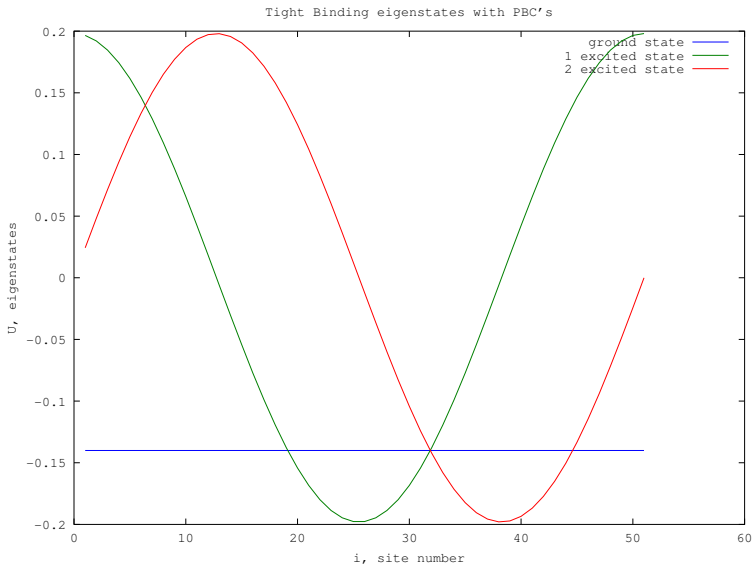

Figure 1: Tight Binding ground, 1^{st} excited and 2^{nd} excited eigenstates with periodic boundry conditions

Fig 0.1 indicates the first three eigenstates with lowest energies of Tight Binding Hamiltonian Eq 1 with periodic boundry conditions.

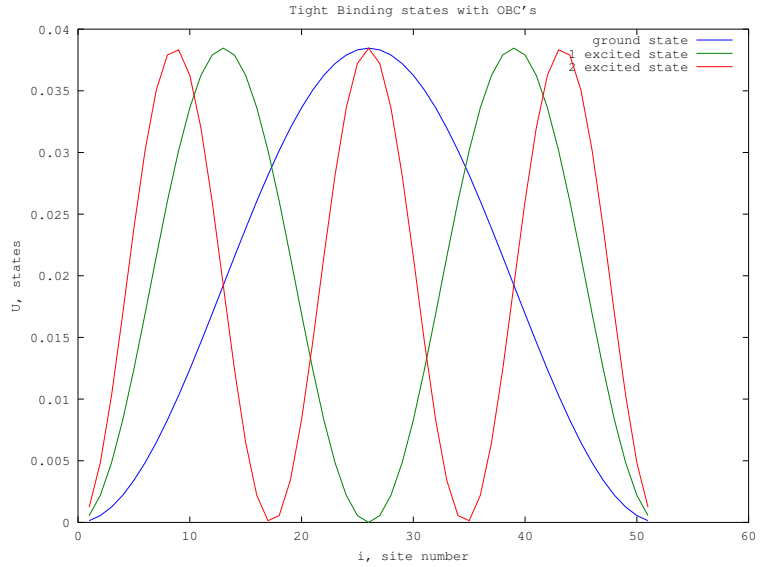

Figure 2: Tight Binding ground, 1^{st} excited and 2^{nd} excited states with hard wall boundry conditions

Ground, 1^{st} excited and 2^{nd} excited states of Tight Binding Hamiltonian 1 are indicated in Fig 2 in the case of hard wall boundry conditions. These states are the thermodynamic limit of the particle in a box eigenstates.

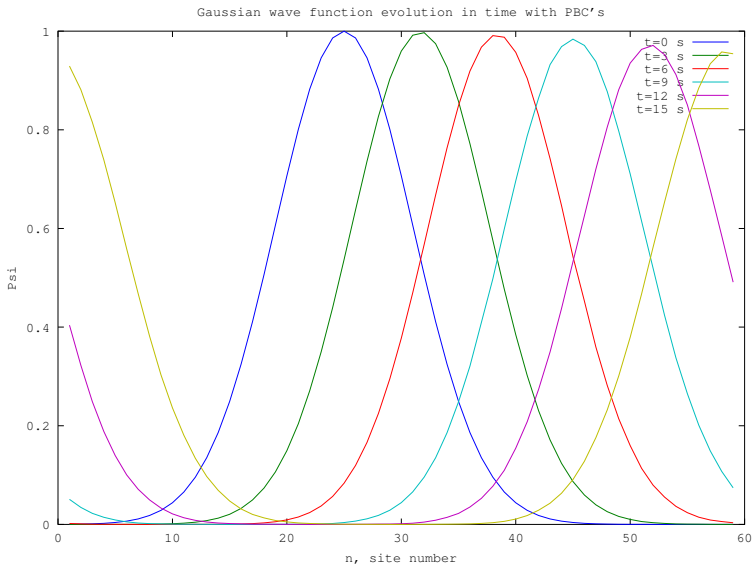

Figure 3: Time dependence of a Gaussian wave function on the Tight Binding chain with PBC's

Starting the time evolution of the system from an initially a Gaussian state,

$$\Psi(x, t = 0) = e^{(x-25)^2/12^2 - ikx} \tag{15}$$

which is not an eigenstate of the Tight Binding Hamiltonian Eq 1, we obtained Fig 0.1. As time evolves shape of the Gaussian wave packets gets wider and shorter. When time reaches $t = 12s$, probability of being at the

head of the chain of the particle which is at the end of the chain rises because of the periodicity of the boundries.

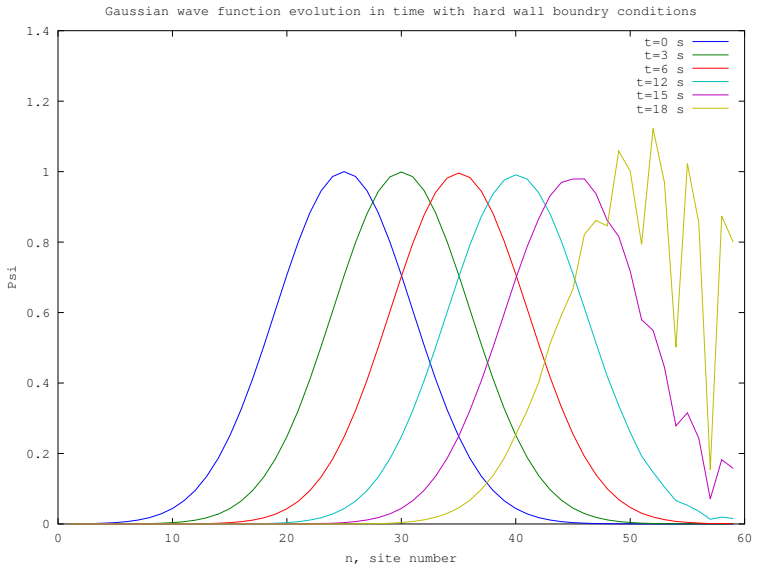

Figure 4: Time dependence of a Gaussian wave function on the Tight Binding chain with the hard wall boundry conditions

A time dependent wave function application of the hard wall boundry conditions in Tight Binding model is demonstrated in Fig 0.1 by using Eq 15 as initial state. Particle can not pass through the hard walls, therefore

Gaussian wave packet deformes at the edge of the chain.

0.2 Bose Hubbard Model

In the Bose Hubbard Model particles can move from one site to a nearest neighboring site via hopping. Repulsive on site interaction prevents sites from double or more occupancy and the chemical potential controls the number of particles throughout the chain. Hamiltonian is given by

$$H = -J \sum_{i=1}^{M-1} (a_i^\dagger a_{i+1} + a_i a_{i+1}^\dagger) + \frac{U}{2} \sum_{i=1}^{M} n_i(n_i - 1) - \mu \sum_{i=1}^{M} n_i \tag{16}$$

where $a_i^\dagger$ and a_{i+1} are the creation and annihilation operators on sites i and $i+1$ respectively and $n_i = a_i^\dagger a_i$ is the number of particles on site i.

In the case $J = 0$ and $\mu = 0$ in Eq 16, minimization of on site interaction to the particle number in Eq 17

$$\frac{\partial \left(\frac{U}{2} n_i(n_i - 1)\right)}{\partial n_i} = 0 \tag{17}$$

gives $n_i = \frac{1}{2}$ which is called as half filling.

Physics of the Bose Hubbard Model arises from the competition between the kinetic J and the potential U terms.

0.2.1 Strong Interaction Regime ($J \ll U$)

For a given chemical potential and on site interaction Bose Hubbard Hamiltonian becomes in the case of $J = 0$

$$H = \frac{U}{2} \sum_{i=1}^{M} n_i(n_i - 1) - \mu \sum_{i=1}^{M} n_i \tag{18}$$

Applying Eq 18 to the Schrodinger Equation energy eigenvalues are found for a definite particle number as in the following.

$$n = 0 \qquad E = 0 \tag{19}$$
$$n = 1 \qquad E = -\mu \tag{20}$$
$$n = 2 \qquad E = U - 2\mu \tag{21}$$
$$n = 3 \qquad E = 3U - 3\mu \tag{22}$$
$$\vdots \qquad \vdots \tag{23}$$
$$n \quad E = \frac{U}{2} n(n-1) - \mu n \tag{24}$$

In this regime particles are localized on the sites, their wavefunction has a product form. This is so called Mott insulator phase. Energy eigenstates of the Eq (18) is given by

$$|\psi\rangle_{MI} = \prod_{i=1}^{M} (b_i^\dagger)^{N/M} |0\rangle \tag{25}$$

0.2.2 Weak Interaction Regime ($U \ll J$)

Taking $U = 0$ in Eq (16) and for a definite chemical potential μ Bose Hubbard Hamiltonian becomes

$$H = -J \sum_{i=1}^{M-1} (a_i^\dagger a_{i+1} + a_i a_{i+1}^\dagger) - \mu \sum_{i=1}^{M} n_i \tag{26}$$

In this case the particles can tunnel from from one site to another via hopping term so that they are delocalized in space. This regime is so called superfluid phase. The energyeigenstates of the Eq (26) are given by

$$|\psi\rangle_{SF} = \prod_{i=1}^{M} \sum_{j=1}^{N} a_j^\dagger |0\rangle \tag{27}$$

According to Eq (27) superfluid wave function is a product of superpositions of different number of particles in each site on the lattice.

0.3 Dicke Model

Interaction between a two level system (TLS) and quantized multimode electromagnetic radiation is described by the Hamiltonian

$$H = \sum_k \epsilon_k a_k^\dagger a_k + \frac{\Omega}{2} \sigma_z + \sum_k V_k (\sigma^+ a_k + \sigma^- a_k^\dagger) \tag{28}$$

where $a_k^\dagger$ (a_k) bosonic creation (annihilation) operator for the cavity photons with momentum k and σ^+ (σ^-) atomic rising (lowering) operators.

It is more convenient to write the Hamiltonian in real space, taking the Fourier transform of the creation and annihilation operators.

$$H = -J\sum_{x=1}^{N}(a_{x+1}^\dagger a_x + h.c.) + \frac{\Omega}{2}\sigma_z + V(\sigma^+ a_{x_0} + h.c.) \tag{29}$$

where x_0 is the location of the TLS on the chain. We consider that the interaction constant between photons and TLS is mode independent ($V_k = V$). The number of the modes in the momentum space is equal to the number of the sites in the real space.

The second part of the Hamiltonian describes the TLS with parameter Ω which is the frequency difference between the two levels.

The third part of the Hamiltonian is for the interaction between the photons and the TLS in which there is photon exchange process among the photon bath and the TLS.

The quantum state that there is no any photon in the cavity and the TLS is in the ground state is **vacuum state**, $|0,-\rangle$. Hence, photon number in the system is the excitation number of the vacuum.

Consider the excitation number in the system is N. When the TLS in its ground state $|-\rangle$, there is N photon in the cavity. A photon lessens by one from the cavity when the atom is in the excited state $|+\rangle$. The excitation number is conserved in this way.

Let us indicate this argument in a fancy way. N photon Fock state with M sites $|N\rangle = |n_1 n_2 \cdots n_{x_0} \cdots n_M\rangle$, so

$$a_{x_0}\sigma^+ |n_1 n_2 \cdots n_{x_0} \cdots n_M, -\rangle = \sqrt{n_{x_0}}\, |n_1 n_2 \cdots n_{x_0} - 1 \cdots n_M, +\rangle \tag{30a}$$

$$a_{x_0}^\dagger\sigma^- |n_1 n_2 \cdots n_{x_0} \cdots n_M, +\rangle = \sqrt{n_{x_0}+1}\, |n_1 n_2 \cdots n_{x_0} + 1 \cdots n_M\rangle \tag{30b}$$

N excitation Fock Space

Let N be the excitation number and M be the number of sites (number of modes) in the chain. The number of the basis vectors spanning N excitation Hilbert space ($\mathcal{H}_N$) is the dimension of the Hilbert space. Hilbert space of the system is simply a direct sum of N photon Hilbert space when the TLS in the ground state ($|-\rangle$) and $N-1$ photon Hilbert space when the TLS in the excited state ($|+\rangle$).

$$\mathcal{H} = \mathcal{H}_N \oplus \mathcal{H}_{N-1} \tag{31}$$

where the Hilbert space $\mathcal{H}$ of the composite system is spanned by the vectors

$$\mathcal{H} = \{|N, -\rangle, |N-1, +\rangle\} \tag{32}$$

Consider we put N photons into a box with M divisions so that there is a M different location for each photon. We can think this as permutation between N photons and $M-1$ walls. There are $N+M-1$ objects to permute.

Dimension of the Hilbert space ($\mathcal{H}_N$) of the N photons for M sites is given by the formula

$$D_N = \frac{(N+M-1)!}{N!(M-1)!} = \binom{N+M-1}{M-1} \tag{33}$$

corresponding to choosing $M-1$ walls from $N+M-1$ objects.

Similarly $N-1$ photon Hilbert space ($\mathcal{H}_{N-1}$) dimension is given by D_{N-1}, replacing $N-1$ by N in Eq 33.

Then, composite system dimension is

$$D = D_N + D_{N-1} \tag{34}$$

0.4 Numerical Implementation

0.4.1 Fock Space Basis Formation

Let us line up $N+M-1$ objects consisting of photons and walls and enumerate positions of each object starting from 1 to $N+M-1$. Different wall positions combinations are found by the formula

$$p = \binom{\overline{N+M-1}}{M-1} \tag{35}$$

where $\overline{N+M-1} = [1 \quad 2 \quad 3 \quad \cdots \quad N+M-1]$ is a row vector. p is also a row vector with $M-1$ columns corresponding to wall positions. Number of photons in each division can be found simply by

$$\begin{array}{lcl} n_1 & = & p_1 - 1 \\ \vdots & \vdots & \vdots \\ n_i & = & p_i - p_{i-1} - 1 \\ \vdots & \vdots & \vdots \\ n_M & = & \overline{N+M-1} - p_{M-1} \end{array}$$

as a row vector. We keep the excitation number information for M site chain by a decimal using the Matlab function **bi2de** as in Table 1. In Appendix A.1 we give the information about *bi2de* function.

	Fock State	vector			decimal	state index
	$\|N;-\rangle$ / $\|N-1;+\rangle$	3^0	3^1	3^2	d	i'
$\mathcal{H}_N$ space vectors	$\|0\ 0\ 2;\ -\rangle$	0	0	2	18	1
	$\|0\ 1\ 1;\ -\rangle$	0	1	1	12	2
	$\|1\ 0\ 1;\ -\rangle$	1	0	1	10	3
	$\|0\ 2\ 0;\ -\rangle$	0	2	0	6	4
	$\|1\ 1\ 0;\ -\rangle$	1	1	0	4	5
	$\|2\ 0\ 0;\ -\rangle$	2	0	0	2	6
$\mathcal{H}_{N-1}$ space vectors	$\|0\ 0\ 1;\ +\rangle$	0	0	1	9	7
	$\|0\ 1\ 0;\ +\rangle$	0	1	0	3	8
	$\|1\ 0\ 0;\ +\rangle$	1	0	0	1	9

Table 1: Decimal representation of $N = 2$ excitation states with $M = 3$ sites when the TLS is in the ground state and excited state. Fock state vectors are converted to a decimal by the Matlab function *bi2de* which does basis arithmetic.

0.4.2 Formation of the Matrix Elements

0.4.3 Tight Binding Hamiltonian

In order to form matrix representation of the Tight Binding Hamiltonian, we firstly obtain the Fock states in a given excitation number N and mode M as explained the previous subsection. The Tight Binding Hamiltonian is given by Eq 1. We choose sites with nonzero occupation and annihilate a photon from them and create in the next sites of them. Clearly, the decimal representing the Fock states are altered by the hopping. This change can be calculated as

$$d' = d - (N+1)^{(j-1)} + (N+1)^j \tag{36}$$

in $N+1$ basis where j is the site number from left side. d' is the representation of the new Fock state and is equal to one of the Fock state vector representations in the Hilbert space. We look for Fock state representation which is equal to d' so that we take the Fock state as the new Fock state. Accordingly, the Tight Binding Hamiltonian matrix elements is obtained by

$$a_x a^\dagger_{x+1}(i', d') = \sqrt{n(j)(n(j)+1)} \tag{37}$$

where i' is the index of the Fock state vector in Table 1 and j is the site number.

According to the Table 2 and Eq 37, we form the matrix as

state index	n			d	$d' = d - (N+1)^{(j-1)} + (N+1)^j$	new state index
1	0	0	2	18		
2	0	1	1	12	$18 = 12 - 3^1 + 3^2$	1
3	1	0	1	10	$12 = 10 - 3^0 + 3^1$	2
4	0	2	0	6	$12 = 6 - 3^1 + 3^2$	2
5	1	1	0	4	$6 = 4 - 3^0 + 3^1$	4
6	2	0	0	2	$4 = 2 - 3^0 + 3^1$	5

Table 2: Table shows change of the states of hopping a photon from one site to its next site. Last column indicates obtained state index after hopping.

$$a_x a_{x+1}^\dagger = \begin{pmatrix} 0 & 0 & 0 & 0 & 0 & 0 \\ \sqrt{2} & 0 & 0 & 0 & 0 & 0 \\ 0 & \sqrt{2} & 0 & 0 & 0 & 0 \\ 0 & 1 & 0 & 0 & 0 & 0 \\ 0 & 0 & 0 & 1 & 0 & 0 \\ 0 & 0 & 0 & 0 & \sqrt{2} & 0 \end{pmatrix} \tag{38}$$

Tight Binding matrix is simply a matrix sum of Eq 38 by its complex conjugate.

$$H_{TB} = \begin{pmatrix} 0 & \sqrt{2} & 0 & 0 & 0 & 0 \\ \sqrt{2} & 0 & \sqrt{2} & 1 & 0 & 0 \\ 0 & \sqrt{2} & 0 & 0 & \sqrt{2} & 0 \\ 0 & 1 & 0 & 0 & 1 & 0 \\ 0 & 0 & \sqrt{2} & 1 & 0 & \sqrt{2} \\ 0 & 0 & 0 & 0 & \sqrt{2} & 0 \end{pmatrix} \tag{39}$$

0.4.4 Interaction Hamiltonian

We continiue the example $N = 2$, $M = 3$ states. When the TLS is excited there is $N - 1 = 1$ photon in the cavity. Assume that TLS is localized in the next of the site labelled by x_0. TLS emits a photon to the cavity, so the occupation number on the site x_0 is increased by 1. This new Fock state coincides up one of the $|N, -\rangle$ states. In order to find the correspondence of it, we calculate the decimal representation of the state by *bi2de*. Table summarizes the explanations above.

$\sigma^- a_{x_0}^\dagger$ matrix elements are founded by

$$\sigma^- a_{x_0}^\dagger(i,j) = \sqrt{n(x_0)+1} \tag{40}$$

d	$\mathcal{H}_{N-1}$ states			state index	new state			d'	state index in $\mathcal{H}_N space$
	3^0	3^1	3^2		3^0	3^1	3^2		
9	0	0	1	7	0	1	1	12	2
3	0	1	0	8	0	2	0	6	4
1	1	0	0	9	1	1	0	4	5

Table 3: $\mathcal{H}_N$ and $\mathcal{H}_{N-1}$ space states correspondance

where i is the order number of the corresponding state in the $\mathcal{H}_N$ space and j is the order number of the Fock state in $\mathcal{H}_{N-1}$ space.

Interaction Hamiltonian is sum of the Eq 40 with its complex conjugate.

0.5 Fixed Chemical Potential

Consider that each site can take at most N particles so that possible number of particles in a single site is $\{0, 1, 2, \cdots, N\}$. Let us to study on a specific example to determine the matrix elements of Bose-Hubbard Hamiltonian in the case of the fixed chemical potential. For the simplicity we choose $N = 2$ and $M = 2$ so that the possible Fock state vectors are given by

	Fock State	vector		decimal	state index
	$\|N\rangle$	3^0	3^1	d	i'
$\mathcal{H}_N$ space vectors	$\|0 \quad 0\rangle$	0	0	0	1
	$\|1 \quad 0\rangle$	1	0	1	2
	$\|2 \quad 0\rangle$	2	0	2	3
	$\|0 \quad 1\rangle$	0	1	3	4
	$\|1 \quad 1\rangle$	1	1	4	5
	$\|2 \quad 1\rangle$	2	1	5	6
	$\|0 \quad 2\rangle$	0	2	6	7
	$\|1 \quad 2\rangle$	1	2	7	8
	$\|2 \quad 2\rangle$	2	2	8	9

Table 4: Decimal representation of $N = 2$ excitation states with $M = 2$ sites. Fock state vectors are converted to a decimal by the Matlab function *bi2de* which does basis arithmetic.

Matrix elements of the Bose-Hubbard Hamiltonian with the basis in Table 4 as in the following:

$$H = \begin{pmatrix} 0 & 0 & 0 & 0 & 0 & 0 & 0 & 0 & 0 \\ 0 & -\mu & 0 & -J & 0 & 0 & 0 & 0 & 0 \\ 0 & 0 & U-2\mu & 0 & -J\sqrt{2} & 0 & 0 & 0 & 0 \\ 0 & -J & 0 & -\mu & 0 & 0 & 0 & 0 & 0 \\ 0 & 0 & -J\sqrt{2} & 0 & -2\mu & 0 & 0 & 0 & 0 \\ 0 & 0 & 0 & 0 & 0 & U-3\mu & 0 & -2J & 0 \\ 0 & 0 & 0 & 0 & -J\sqrt{2} & 0 & U-2\mu & 0 & 0 \\ 0 & 0 & 0 & 0 & 0 & -2J & 0 & U-3\mu & 0 \\ 0 & 0 & 0 & 0 & 0 & 0 & 0 & 0 & 2U-4\mu \end{pmatrix}$$

Chapter 1

Density Matrix Renormalization Group (DMRG)

1.1 Wave Function Transformation

Transforming the wave function while updating the left block

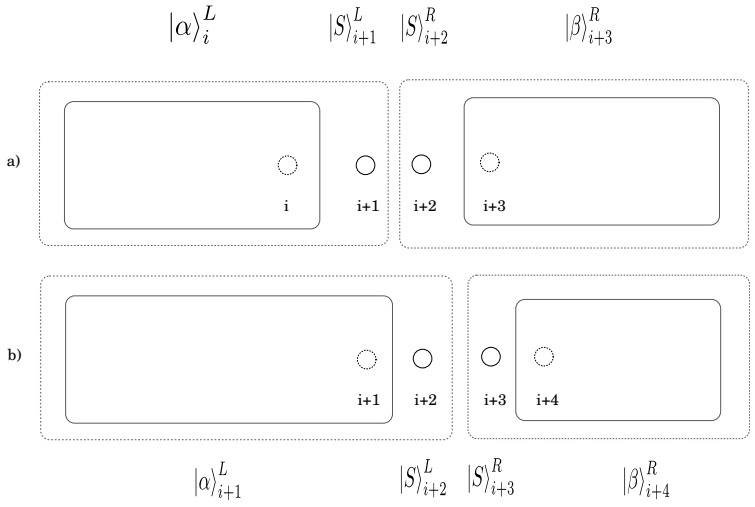

Figure 1.1: Direct product structure of the product basis of the super-block in left to right sweep step, i indicates the rightmost site of the left block. Note that $S_{i+2}^R \rightarrow S_{i+2}^L$ in (b)

According to Fig 1.1, super-block ground state wave functions are written as

$$|\psi_i\rangle = \sum_{\alpha_i^L S_{i+1}^L S_{i+2}^R \beta_{i+3}^R} \psi(\alpha_i^L S_{i+1}^L S_{i+2}^R \beta_{i+3}^R)\, |\alpha_i^L\rangle \otimes |S_{i+1}^L\rangle \otimes |S_{i+2}^R\rangle \otimes |\beta_{i+3}^R\rangle \tag{1.1a}$$

where $\psi(\alpha_i^L S_{i+1}^L S_{i+2}^R \beta_{i+3}^R)$ represents the coefficients in the tensor product basis in the i^{th} position, $\{|\alpha_i\rangle\}$ the left block basis, $\{|\beta_j\rangle\}$ the right block basis and $\{|S_i^L\rangle\}$, $\{|S_j^R\rangle\}$ the left and the right central site basis. The decomposition in the next step will be written as

$$|\tilde{\psi_{i+1}}\rangle = \sum_{\alpha_{i+1}^L S_{i+2}^L S_{i+3}^R \beta_{i+4}^R} \psi(\alpha_{i+1}^L S_{i+2}^L S_{i+3}^R \beta_{i+4}^R)\, |\alpha_{i+1}^L\rangle \otimes |S_{i+2}^L\rangle \otimes |S_{i+3}^R\rangle \otimes |\beta_{i+4}^R\rangle \tag{1.1b}$$

which will be approximate initial guess for the *eigs* function. We will find how to pass from Eq 1.1a to Eq 1.1b. When the sweep direction is left to right as in Fig 1.1, the active block is the left block, so the free site of the right block becomes the free site of the left block in the new basis. It means that the state vector of S_{i+2}^L is not subjected to any operation while the left block state vector and the right block state vector are transformed to the new basis by the transformation matrices O_L and O_R, respectively. This can be done as in the following:

Using the completeness relation for the new basis

$$\sum_{\alpha_{i+1}^L S_{i+2}^L S_{i+3}^R \beta_{i+4}^R} |\alpha_{i+1}^L S_{i+2}^L S_{i+3}^R \beta_{i+4}^R\rangle \langle \alpha_{i+1}^L S_{i+2}^L S_{i+3}^R \beta_{i+4}^R| \approx \mathbb{I} \tag{1.2}$$

Eq 1.2 is placed in Eq 1.1a, the relation between the wave vector coefficients in old and new basis is found as

$$\psi(\alpha_{i+1}^L S_{i+2}^L S_{i+3}^R \beta_{i+4}^R) \approx \sum_{\alpha_i^L S_{i+1}^L S_{i+2}^R \beta_{i+3}^R} \psi(\alpha_i^L S_{i+1}^L S_{i+2}^R \beta_{i+3}^R) \times \langle \alpha_{i+1}^L S_{i+2}^L S_{i+3}^R \beta_{i+4}^R | \alpha_i^L S_{i+1}^L S_{i+2}^R \beta_{i+3}^R \rangle \tag{1.3}$$

where the inner products can be written as

$$\langle \alpha_{i+1}^L S_{i+2}^L S_{i+3}^R \beta_{i+4}^R | \alpha_i^L S_{i+1}^L S_{i+2}^R \beta_{i+3}^R \rangle = \underbrace{\langle \alpha_{i+1}^L | \alpha_i^L S_{i+1}^L \rangle}_{O_L^\dagger(\alpha_i^L S_{i+1}^L, \alpha_{i+1}^L)} \underbrace{\langle S_{i+2}^L | S_{i+2}^R \rangle}_{\delta_{S_{i+2}^L, S_{i+2}^R}} \underbrace{\langle S_{i+3}^R \beta_{i+4}^R | \beta_{i+3}^R \rangle}_{O_R(S_{i+3}^R \beta_{i+4}^R, \beta_{i+3}^R)} \tag{1.4}$$

so that

$$\psi(\alpha^L_{i+1}S^L_{i+2}S^R_{i+3}\beta^R_{i+4}) \approx \sum_{\alpha^L_i S^L_{i+1} S^R_{i+2}\beta^R_{i+3}} \psi(\alpha^L_i S^L_{i+1} S^R_{i+2}\beta^R_{i+3})\times O^\dagger_L(\alpha^L_i S^L_{i+1}, \alpha^L_{i+1})\delta_{S^L_{i+2},S^R_{i+2}} O_R(S^R_{i+3}\beta^R_{i+4}, \beta^R_{i+3}) \tag{1.5}$$

As we need to transform ground state vector of the i^{th} super-block configuration from left to the next step by transforming the left part and the right part of the state vector separately, it is convenient to write super-block state vector in Eq 1.1a in matrix form instead of doing a tensor product decomposition. We use the *reshape* command to transform a Nx1 vector to a n_Lxn_R matrix, where $n_L n_R = N$. Explicitely,

$$U\left|\psi_0\right\rangle = U_L\left|\psi^L_0\right\rangle \otimes U_R\left|\psi^R_0\right\rangle \tag{1.6}$$

where $U = U_L \otimes U_R$ some operator which transforms the wave vector and $U_L = O^\dagger_R$, $U_R = (\mathbb{I} \otimes O_R)$. Let us write the matrix form of the wave vector as $\psi_{\mathbf{0}} = \left|\psi_L\right\rangle\left\langle\psi_R\right|$ where $\left\langle\psi^R\right| = \left|\psi^R\right\rangle^\dagger$.

In order to rotate the wavefunction to the new basis in matrix form, operators are simply applied to it as

$$\tilde{\boldsymbol{\psi}}_{\mathbf{0}} = \boldsymbol{O}^\dagger_{\boldsymbol{L}}\boldsymbol{\psi}_{\mathbf{0}}(\mathbb{I} \otimes \boldsymbol{O}_{\boldsymbol{R}})^\dagger \tag{1.7}$$

when sweeping from left to right providing the Eq 1.5.

The use of formula Eq A.6 is explained in the Appendix with the *reshape* command.

Transforming the wave function while updating the right block

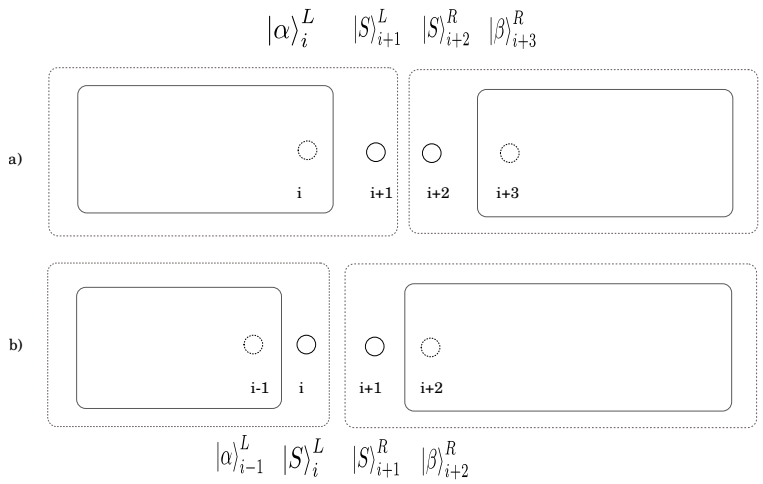

Figure 1.2: Direct product structure of the product basis of the super-block in right to left sweep step, i indicates the rightmost site of the left block. Note that $S_{i+1}^L \rightarrow S_{i+1}^R$ in (b)

Let us now to indicate how to do the wave function transformation when the direction of the sweep is switched to the left (updating right block). According to the Fig 1.2, the initial index of the left block is i which is the same as Fig 1.1-a whose wave function in the product basis is represented by Eq 1.1a.

We do transfrom the wave function Eq 1.1a to the new basis given by

$$|\tilde{\psi_{i-1}}\rangle = \sum_{\alpha_{i-1}^L S_i^L S_{i+1}^R \beta_{i+2}^R} \psi(\alpha_{i-1}^L S_i^L S_{i+1}^R \beta_{i+2}^R) \, |\alpha_{i-1}^L\rangle \otimes |S_i^L\rangle \otimes |S_{i+1}^R\rangle \otimes |\beta_{i+2}^R\rangle \tag{1.8}$$

by using the completeness property of the new basis

$$\sum_{\alpha_{i-1}^L S_i^L S_{i+1}^R \beta_{i+2}^R} |\alpha_{i-1}^L S_i^L S_{i+1}^R \beta_{i+2}^R\rangle \, \langle \alpha_{i-1}^L S_i^L S_{i+1}^R \beta_{i+2}^R| \approx \mathbb{I} \tag{1.9}$$

in Eq 1.1a, we obtain the final state coefficients as

$$\Psi(\alpha^L_{i-1}S^L_i S^R_{i+1}\beta^R_{i+2}) \approx \sum_{\alpha^L_i S^L_{i+1} S^R_{i+2}\beta^R_{i+3}} \psi(\alpha^L_i S^L_{i+1} S^R_{i+2}\beta^R_{i+3})\times \\ \langle \alpha^L_{i-1}S^L_i S^R_{i+1}\beta^R_{i+2} | \alpha^L_i S^L_{i+1} S^R_{i+2}\beta^R_{i+3}\rangle \tag{1.10}$$

in terms of the old state coefficients. We rewrite the last expression as

$$\Psi(\alpha^L_{i-1}S^L_i S^R_{i+1}\beta^R_{i+2}) \approx \sum_{\alpha^L_i S^L_{i+1} S^R_{i+2}\beta^R_{i+3}} \psi(\alpha^L_i S^L_{i+1} S^R_{i+2}\beta^R_{i+3})\times \\ \underbrace{\langle \alpha^L_{i-1}S^L_i|\alpha^L_i\rangle}_{O_L(\alpha^L_{i-1}S^L_i,\alpha^L_i)} \underbrace{\langle S^R_{i+1}|S^L_{i+1}\rangle}_{\delta_{S^R_{i+1},S^L_{i+1}}} \underbrace{\langle \beta^R_{i+2}|S^R_{i+2}\beta^R_{i+3}\rangle}_{O^\dagger_R(S^R_{i+2}\beta^R_{i+3},\beta^R_{i+2})} \tag{1.11}$$

We prefer to work with the matrix form of the state vector which is $\boldsymbol{\psi_0} = |\psi^L_0\rangle\langle\psi^R_0|$ where $\langle\psi^R_0| = |\psi^R_0\rangle^\dagger$. Consequently, Eq 1.6 in which $U_L = (\boldsymbol{O_L}\otimes\mathbb{I})$ and $U_R = \boldsymbol{O_R}^\dagger$ can be written as

$$\tilde{\boldsymbol{\psi}}_{\mathbf{0}} = (\boldsymbol{O_L}\otimes\mathbb{I})\boldsymbol{\psi_0}\boldsymbol{O_R} \tag{1.12}$$

in the matrix form.

Chapter 2

Time Dependent Density Matrix Renormalizaiton Group Algorithm (tDMRG)

2.1 The Adaptive Time-Dependent DMRG

2.1.1 Suzuki-Trotter Approach

Time evolution of a state $|\psi\rangle$ is done by successive iterations of time evolution operator by δt time-steps as

$$|\psi(t)\rangle = (e^{-iH\delta t} \cdots e^{-iH\delta t}) |\psi(0)\rangle \tag{2.1}$$

where H could be written as a sum of local bond Hamiltonian operators

$$H = H_1 + H_2 + \cdots + H_{N-1} \tag{2.2}$$

in which N is the number of sites on the chain.

Each local bond Hamiltonian $H_1, H_2, \cdots, H_{N-1}$ involve only the nearest neighbor interactions and do not commute each other if they have a common site. i.e. $[H_i, H_{i+1}] \neq 0$ where i is the site index on the chain. Hence it is not correct to split the time evolution operator as

$$e^{-iH\delta t} \neq e^{-iH_1\delta t} e^{-iH_2\delta t} \cdots e^{-iH_{N-1}\delta t} \tag{2.3}$$

In order to break up the statement in an appropriate way, we group the local bond Hamiltonians as not to have any common sites so that each group consist of commuting local bond Hamiltonians. Let us call to one

group even local bond Hamiltonians; $H_2, H_4, H_6, \cdots$ and the other odd local bond Hamiltonians; $H_1, H_3, H_5, \cdots$. Hence we can split the time evolution operator in terms of the commuting local bond Hamiltonians as

$$e^{-iH_A\delta t} = e^{-iH_2\delta t}e^{-iH_4\delta t}\cdots \tag{2.4a}$$

$$e^{-iH_B\delta t} = e^{-iH_1\delta t}e^{-iH_3\delta t}\cdots \tag{2.4b}$$

where H_A, H_B represent even bond Hamiltonian group and odd bond Hamiltonian group respectively.

In order to evolve whole state of the chain in time, both even and odd local bond Hamiltonians should be in used in time evolution operator. It is given by the second order Suzuki-Trotter expansion which is exactly equal to $e^{-iH\delta t} = 1 - iH\delta t - \frac{H^2}{2!}\delta t^2 + \cdots$ expansion up to the third order terms.

$$e^{-i(H_A+H_B)\delta t} = e^{-iH_A\delta t/2}e^{-iH_B\delta t}e^{-iH_A\delta t/2} + \mathcal{O}(\delta t^3) \tag{2.5}$$

with the $\mathcal{O}(\delta t^3)$ error. Since order of the error decreases by $\mathcal{O}(\delta t^3)$ with δt, it is convenient to use second order expansion and also to evolve the system small δt time-steps.

Let us to show up the above argument in the following paragraphs.

$$\begin{aligned}
e^{-iH_A\delta t/2}e^{-iH_B\delta t}e^{-iH_A\delta t/2} =& (1 - iH_A\delta t - \frac{H_A^2}{2!}\delta t^2 - i\frac{H_A^3}{3!}\delta t^3 + \cdots) \\
&\times (1 - iH_B\delta t - i\frac{H_B^2}{2!}\delta t^2 - i\frac{H_B^3}{3!}\delta t^3 + \cdots) \\
&\times (1 - iH_A\delta t - \frac{H_A^2}{2!}\delta t^2 - i\frac{H_A^3}{3!}\delta t^3 + \cdots) \\
&= 1 - i(H_A + H_B)\delta t - (H_A + H_B)\frac{\delta t^2}{2} \\
&- i\frac{H_A^3}{3!}\frac{\delta t^3}{2^3} - i\frac{H_B^3}{3!}\frac{\delta t^3}{2^3} - i\frac{H_B^3}{3!}\delta t^3 \\
&+ i\frac{H_A H_B^2}{2!}\delta t^3 + i\frac{H_A^2 H_B}{2}\delta t^3 + i\frac{H_1^3}{4}\delta t^3
\end{aligned} \tag{2.6}$$

where $H = H_A + H_B$. The terms which are proportional to the third power of δt (δt^3) are not equal to the third power terms in the $e^{-iH\delta t}$ expansion. Hence we see that the error of the expansion is the order of δt^3 with small time-steps.

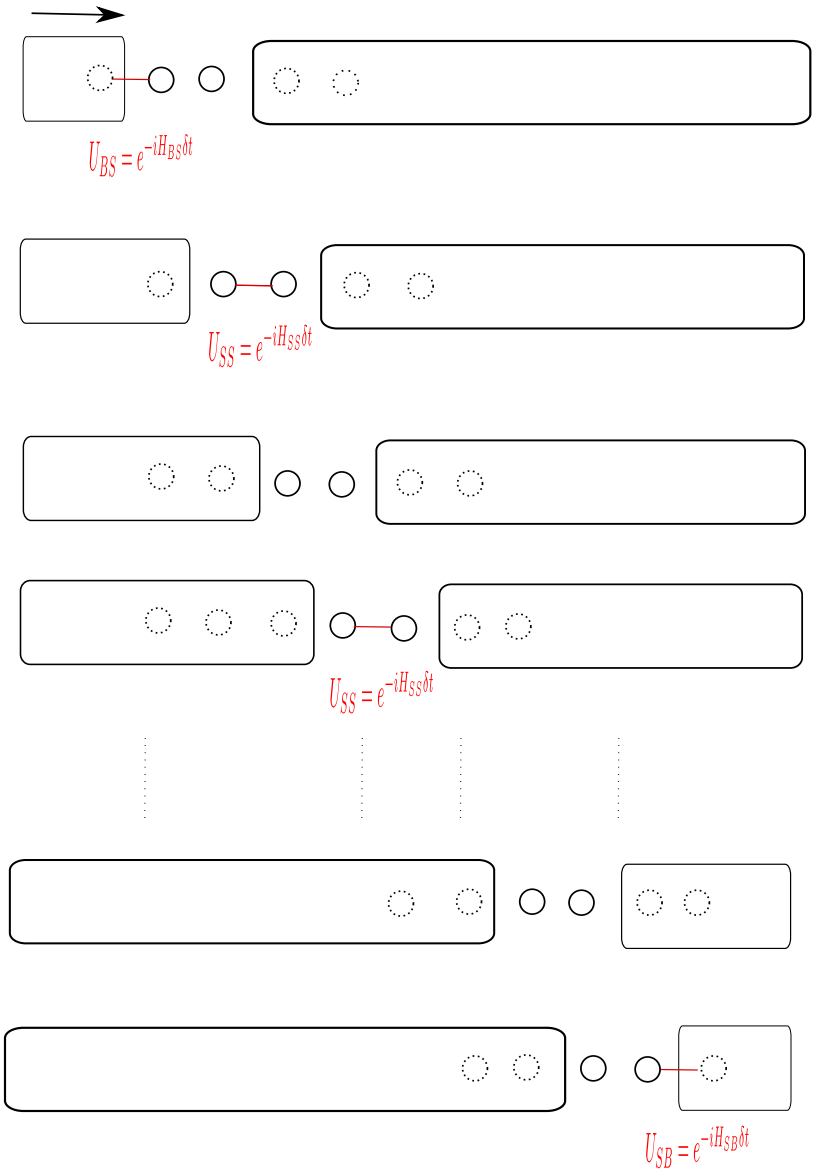

Figure 2.1: Time evolution of bonds while sweeping from left to right. Red lines indicate the bonds which will be evolved in time by a time step δt. U_{BS}, U_{SS}, U_{SB} respectively correspond to block-site bond, site-site bond and site-block bond time evolution operators.

Consider Fig 2.1 where the sweep direction is toward right. We start

applying the time evolution operator from the left block- site bond and continue to apply the time evolution operator every appropriate free site bonds on the chain. Finally, we end up a site-block bond at the last step of the sweep in the right direction. Local bond Hamiltonians in the time evolution operators are

$$\hat{H}_{BS} = -J(\hat{a}_B^\dagger \otimes \hat{a}_S + \hat{a}_B \otimes \hat{a}_S^\dagger) + \frac{U}{2}\left(\mathbb{I}_B \otimes \frac{(\hat{n}(\hat{n}-\mathbb{I}))_S}{2} + \frac{(\hat{n}(\hat{n}-\mathbb{I}))_B}{2} \otimes \mathbb{I}_S\right) \tag{2.7a}$$

$$\hat{H}_{SS} = -J(\hat{a}_S^\dagger \otimes \hat{a}_S + a_S \otimes a_S^\dagger) + \frac{U}{2}\left(\frac{(\hat{n}(\hat{n}-\mathbb{I}))_S}{2} \otimes \mathbb{I}_S + \mathbb{I}_S \otimes \frac{(\hat{n}(\hat{n}-\mathbb{I}))_S}{2}\right) \tag{2.7b}$$

$$\hat{H}_{SB} = -J(\hat{a}_S^\dagger \otimes \hat{a}_B + \hat{a}_S \otimes \hat{a}_B^\dagger) + \frac{U}{2}\left(\frac{(\hat{n}(\hat{n}-\mathbb{I}))_S}{2} \otimes \mathbb{I}_B + \mathbb{I}_S \otimes \frac{\hat{n}(\hat{n}-\mathbb{I}))_B}{2}\right) \tag{2.7c}$$

in the exact basis (no truncation). Note here that

$$\sum_{i=1}^{ti} \frac{\hat{n}_i(\hat{n}_i - \mathbb{I})}{2} = \frac{(\hat{n}(\hat{n}-\mathbb{I}))_B}{2} \tag{2.8}$$

is a sum over all index in the block which is in the exact basis. We sweep the chain in the right direction only once and twice for in the left direction for the time step δt according to Eq 2.5.

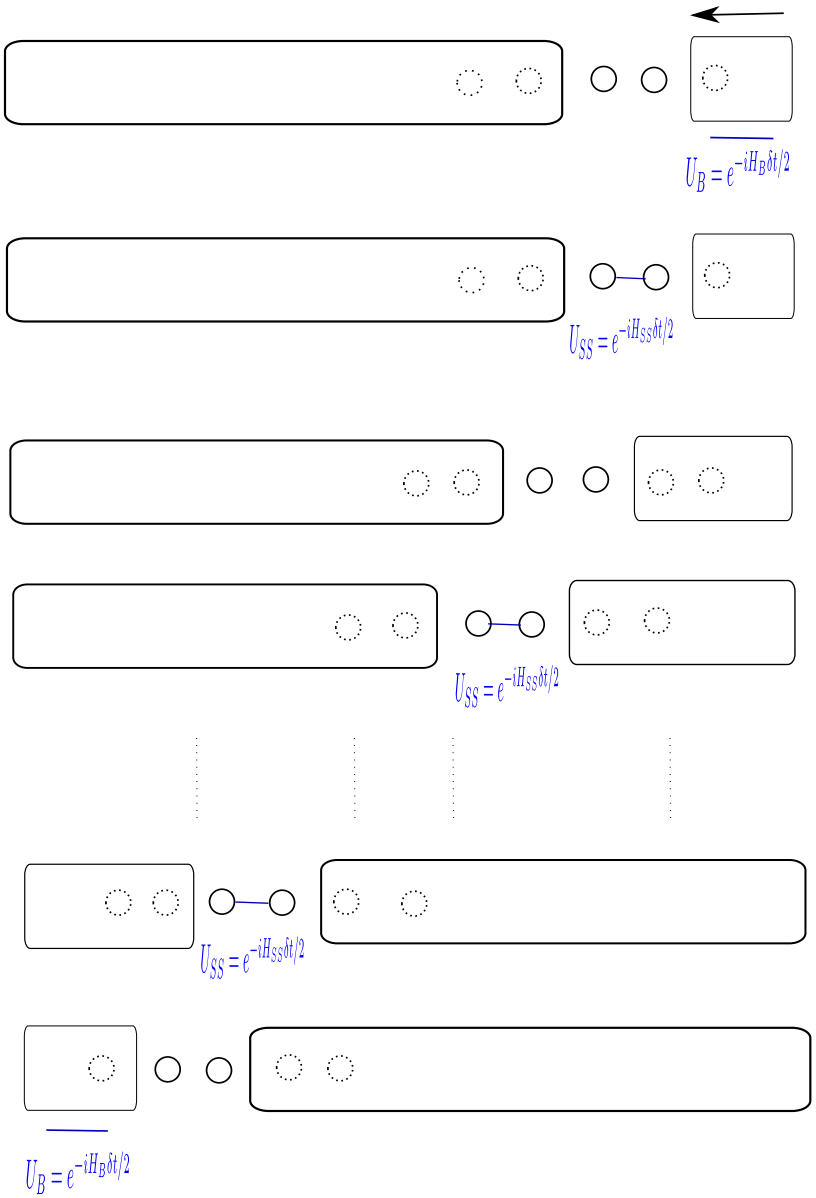

Figure 2.2: Time evolution of the bonds while sweeping from right to left. Blue lines indicate the bonds which will be evolved in time by a time step $\delta t/2$. U_B and U_{SS} correspond to respectively block and site-site bond time evolution operators.

Fig 2.2 shows the evolved bonds in time step by step while the left block being updated. Local bond Hamiltonians which are appropriate to evolve state in time are

$$\hat{H}_B = -J \sum_{i=}^{ti} (\hat{a}_i \otimes \hat{a}_{i+1}^{\dagger} + \hat{a}_i^{\dagger} \otimes \hat{a}_{i+1}) + U \sum_{i=1}^{ti} \left(\frac{\hat{n}_i(\hat{n}_i - \mathbb{I})}{2} \right) \tag{2.9}$$

where ti is the exact site number in the block so that the block is in the exact basis state. H_{SS} is the same with Eq 2.7b. We have already insert the onsite interaction of the blocks by half in Eq (2.7c) and in Eq (2.7a). Therefore we substruct half of the block onsite interactions from the block Hamiltonians in the following way:

$$\hat{H}'_B = \hat{H}_B - \frac{U}{2} \sum_{i=1}^{ti} \left(\frac{\hat{n}_i(\hat{n}_i - \mathbb{I})}{2} \right) \tag{2.10}$$

Chapter 3

DMRG Implementations On Selected Models

3.1 Tight-Binding Model

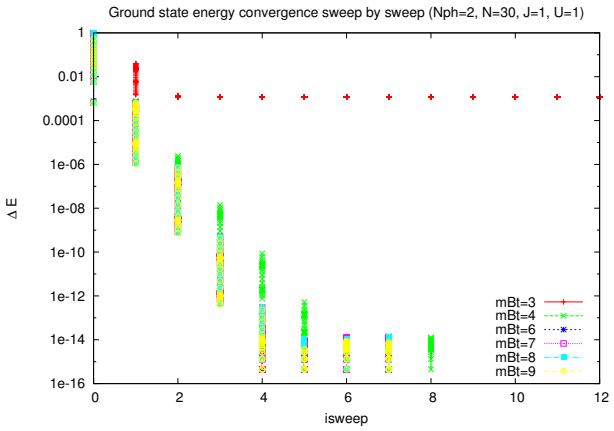

Figure 3.1: Ground state energy convergence comprasion of the Tight Binding Hamiltonian with varying truncation dimensions. There are $N = 2$ photons and $M = 30$ sites on the chain. Vertical dots indicate energy convergence of each site on the chain.

By keeping only the most relevant number of states (m_t)of the block Hamiltonian, we keep $m_t^2 m_s^2$ number of states for the Hilbert space of the superblock system in which m_s is the single site dimension.In Fig 3.1, energy convergence of the ground state for different number of kept states each

block is indicated. For $N = 2$ photons states keeping $m_t = 3$ number of states for blocks is less sufficient for the simulation. Convergence gets better and number of sweeps for the convergence decreases with bigger truncation dimensisons. Therefore, simulation time is decrased.

3.2 Bose-Hubbard Model with Fixed Particle Number

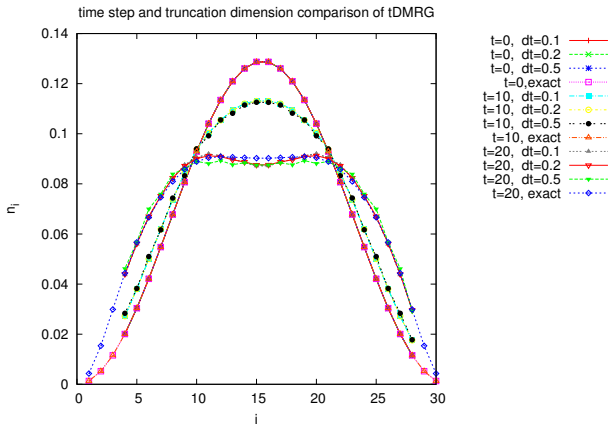

Figure 3.2: Ground state occupation distribution of two photons on Bose-Hubbard lattice with $M = 30$ sites. Figure is a comparison of exact diagonalization results and DMRG with $mBt = 9$ states at different times and time steps.

According to Fig 3.2 ground state particle distributions are superposed at $t = 0$ for a $M = 30$ site chain, just before the time evolution. At $t = 10$, difference between the DMRG and the exact diagonalizaiton results begin to appear and at $t = 20$ this difference becomes more clear even for $dt = 0.1$.

In Fig 3.3, we compare DMRG with different truncation dimensions, mBt besides different time steps, dt to distinguish the relative order of the truncation error and trotter error. To the figure, DMRG with $mBt = 9$ is more close to the exact diagonalization method result. We conclude here that convergence of the ground state wave function is the key point of the DMRG simulation. Suzuki-Trotter error is negligible in these scales if dt is sufficiently small.

Our aim is to cover the Hilbert space of the system by keeping minimum number of particle states. We saw in Fig 3.3 that $mBt = 9$ is not sufficient to

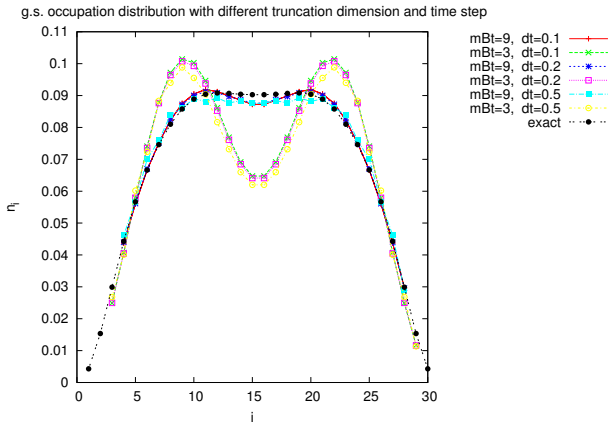

Figure 3.3: Comparison of ground state occupation distribution of two photon Bose-Hubbard lattice at time $t = 20$ with $mBt = 3$ and $mBt = 9$ states for DMRG and exact diagonalization.

achieve this aim for a chain with $M = 30$ sites. Fig 3.4 is created to answer the question that at least how many states is needed to represent the Hilbert space of a specific system with definite dimension. We see from the figure that for a 2 photon Bose-Hubbard lattice with $M = 10$ sites, whose Hilbert space dimension is $D = 55$, $mBt = 5$ and less is not sufficient. Because we only keep $mBt^2 \leq 5^2 = 25$ of these $D = 55$ two photon states. On the other hand, if we attempt to keep more states exceeding the two photon states dimension, these include more than two photon states. DMRG simulations are not compatible with that of exact diagonalization in these cases.

Fig 3.5 indicates the sum of the most weighted eigenvalues of the reduced density matrix during the time evolution algorithm. Here, truncation dimension, $mBt = 40$ fixed. The control parameter is the number of sweeps in finite size DMRG algorithm. We see from the figure that sum of the most weighted eigenvalues is decreasing in time during the simulation, but in a more stabile way in the case of $nsweep = 20$ compared to $nsweep = 6$.

3.3 Bose-Hubbard Model with Fixed Chemical Potential

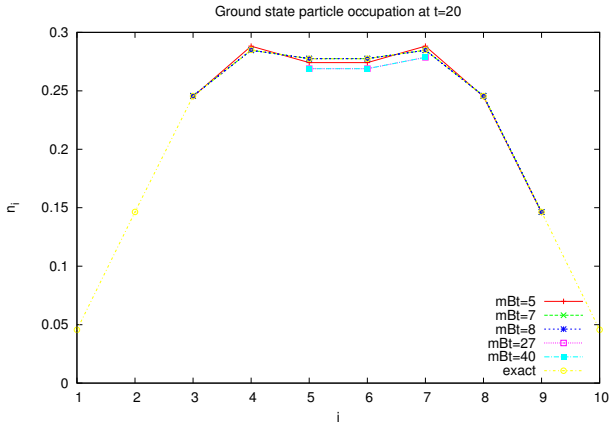

Figure 3.4: Convergence test of ground state via occupation distribution of two photons on Bose-Hubbard lattice with 10 sites.

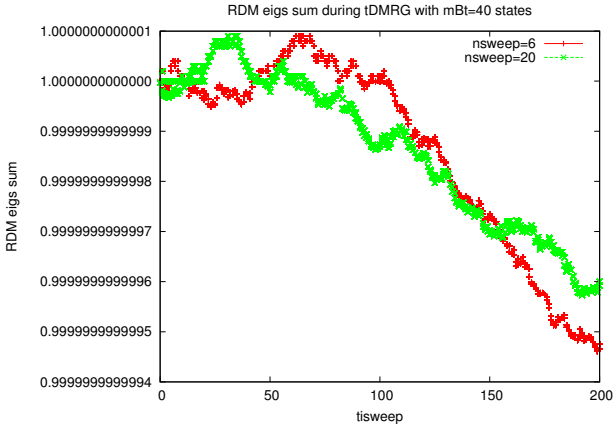

Figure 3.5: Sum of the RDM eigenvalues with fixed truncation dimension changing sweep number

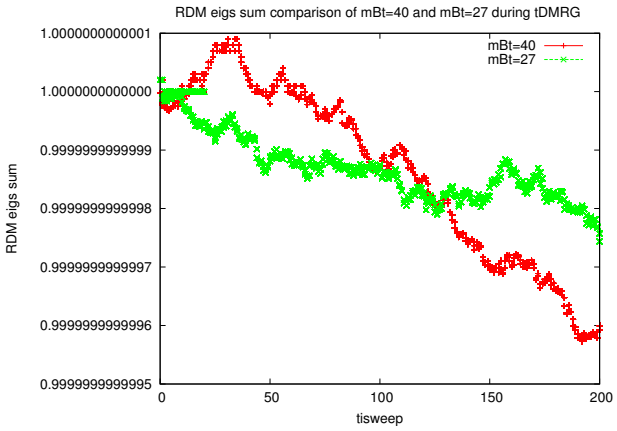

Figure 3.6: Comparison of sum of most weighted reduced density matrix eigenvalues for the $mBt = 40$ and $mBt = 27$ during tDMRG

Appendix A

Matlab functions used in numerical calculations

A.1 bi2de function

bi2de function converts a binary digit vector in a certain basis ($N+1$ or N) to a decimal as below

$$d = bi2de(\overline{n}, N+1) \tag{A.1}$$

To give an example of this, take $N = 1$, $M = 3$ Fock states which are the set of $\{[1 \quad 0 \quad 0]\}$. What `bi2de` does is the basis arithmetic for the $\overline{n}$ in basis N from right side by default. Therefore the biggest element of the $\overline{n}$ is smaller than N.

The machine that we run Dicke programme keeps on memory and operates on decimals with at most 19 (nineteen) digits. This leads to a restriction on the size of the system that we study on. A decimal with 19 digits $10^{18} \approx 2^{59}$. Therefore conversion from a binary to a decimal is not exact for the decimals having more than 59 digits for the single photon case ($N+1 = 2$ basis). It means that one can operate on the system with $M + 1 = 60$ sites exactly in the single photon case. For N photons with M sites, decimal that is converted from binary must be $(N+1)^{M-1} \leq 2^{59}$. This is the maximum value that the computer keeps exactly. Consequently, the number of the sites is restricted to

$$M \leq 59 \log_{N+1}(2) + 1 \tag{A.2}$$

for the excitation number N.

A.2 de2bi function

de2bi function converts a positive decimal to a binary row vector with M columns by typing

$$\overline{n} = de2bi(d, M) \tag{A.3}$$

which does the inverse process of *bi2de*. The number of the digits of the decimal d should not be bigger that 59 for *de2bi* to convert exactly d to binary vector $\overline{n}$.

A.3 *reshape* command and wave function prediction formulas

Consider a $nx1$ column vector with the elements

$$A = \begin{pmatrix} a_{11} \\ a_{21} \\ \vdots \\ a_{n1} \end{pmatrix}_{n,1} \tag{A.4}$$

reshape command changes the column and row sizes of a matrix to the given size by $\tilde{A} = reshape(A, l, m)$ where l expresses the row number and m expresses the column number of the new matrix $\tilde{A}$ and $l * m = n$. The elements of the $\tilde{A}$ are

$$\tilde{A} = \begin{pmatrix} a_{11} & a_{(l+1)2} & \cdots & a_{(ml+1)m} \\ a_{21} & a_{(l+2)2} & \cdots & a_{(ml+2)m} \\ \vdots & \vdots & \cdots & \vdots \\ a_{l1} & a_{(2l)2} & \cdots & a_{(ml)m} \end{pmatrix} \tag{A.5}$$

We transform the wave vector into the matrix form by the *reshape* command which do not have the complex conjugate operation. The complexity of the right block wave function is in the matrix $\tilde{A}$. Therefore, Eq A.6 is used in the DMRG implementation as

$$\tilde{\boldsymbol{\psi}}_{\mathbf{0}} = \boldsymbol{O}_{\boldsymbol{L}}^{\dagger} \boldsymbol{\psi}_{\mathbf{0}} (\mathbb{I} \otimes \boldsymbol{O}_{\boldsymbol{R}})^{T} \tag{A.6}$$

for the left to right sweeping. Similarly, the right to left sweep wave function transformation formula Eq 1.12 is used as

$$\tilde{\boldsymbol{\psi}}_{\mathbf{0}} = (\boldsymbol{O}_{\boldsymbol{L}}^{\dagger} \otimes \mathbb{I}) \boldsymbol{\psi}_{\mathbf{0}} O_R^{*} \tag{A.7}$$

Appendix B

Operator Saving During DMRG Algorithm

B.1 Infinite-size Algorithm

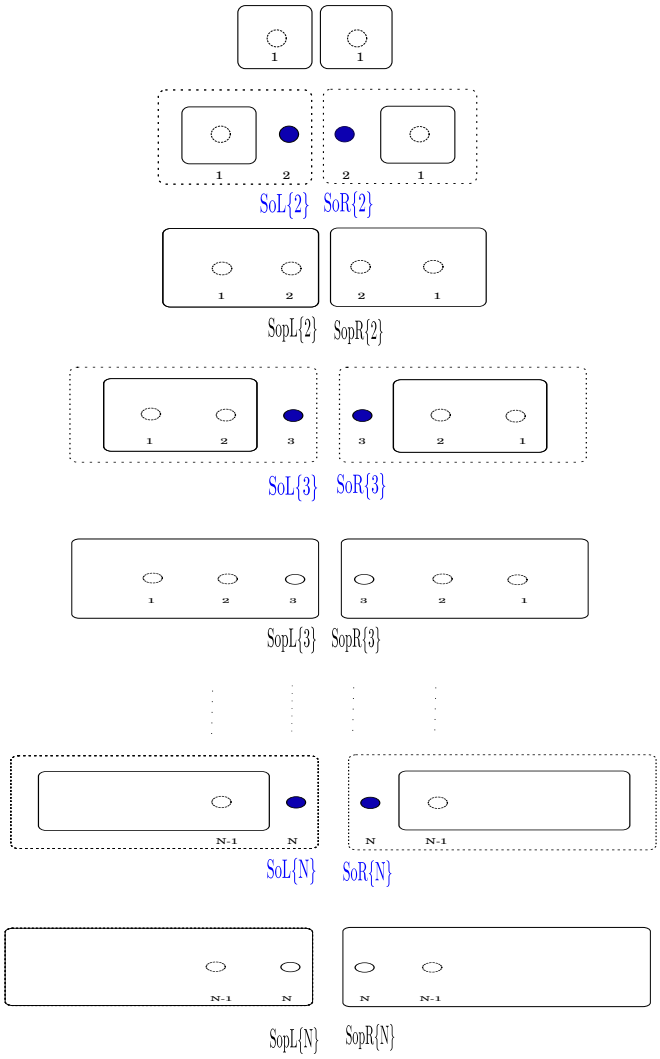

Figure B.1: Turn and index of saving block operators during infinite size algorithm in which left and right blocks are enlarged simultaneously. $SoL\{i\}$ ($SoR\{i\}$) is left block (right block) truncation matrix of the i^{th} enlarged block and $SopL\{i\}$ ($SopR\{i\}$) is the left block (right block) opeators of the i^{th} enlarged block.

B.2 Finite size Algorithm

B.2.1 Sweeping from Left to Right

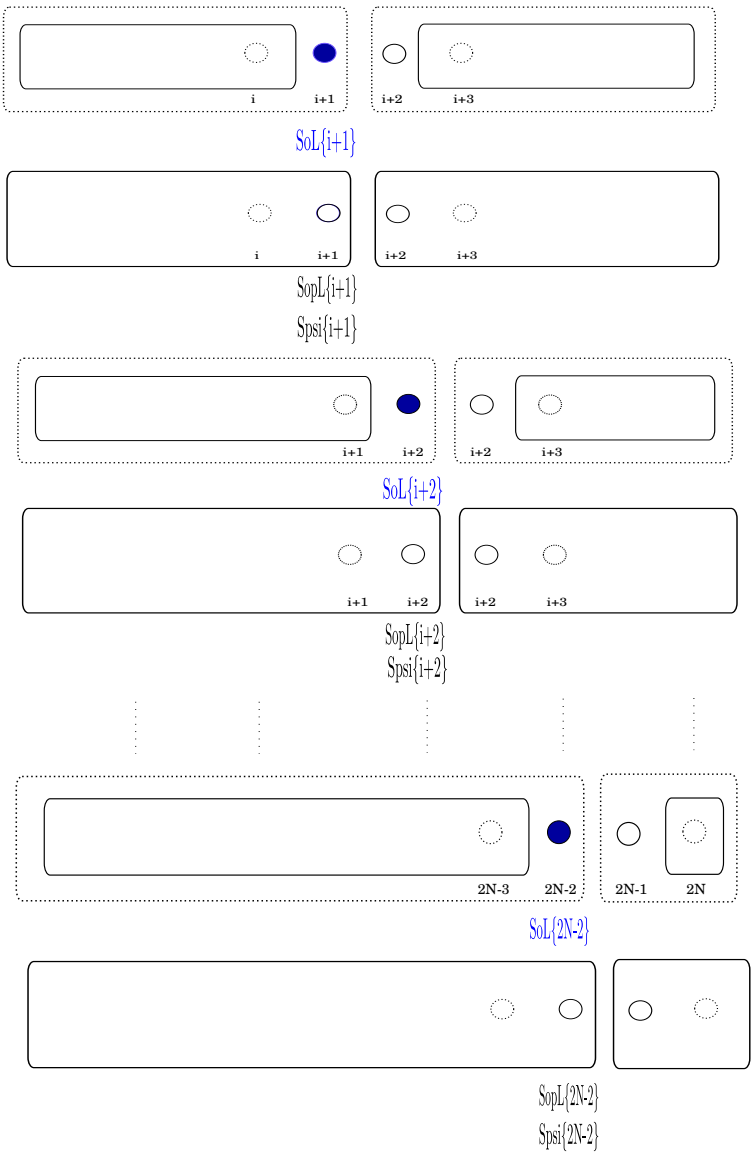

Figure B.2: Left to right sweeping starting from the i^{th} enlargement of the left block to the $2N-1^{th}$ enlargement. Operators are saved by the rightmost site index of the left enlarged blocks.

B.2.2 Sweeping from Right to Left

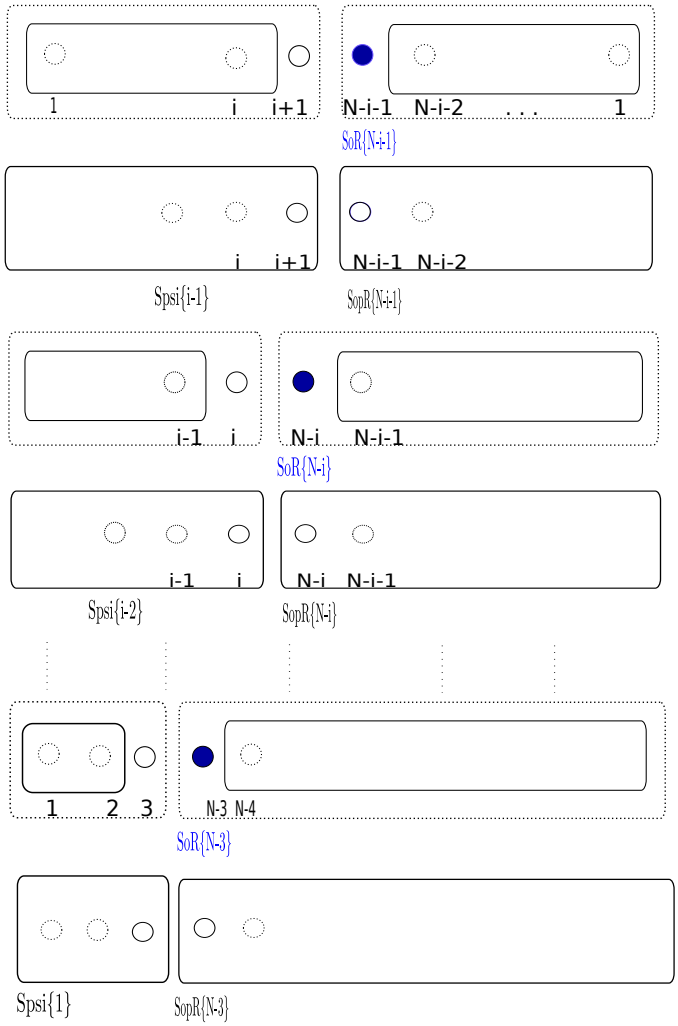

Figure B.3: Right to left sweeping process starting from the $N-i-2^{th}$ enlargement of the right block where i is the rightmost site of the left block. Right block operators are saved by the leftmost index of the right enlarged block.

B.2.3 Wave Function Prediction

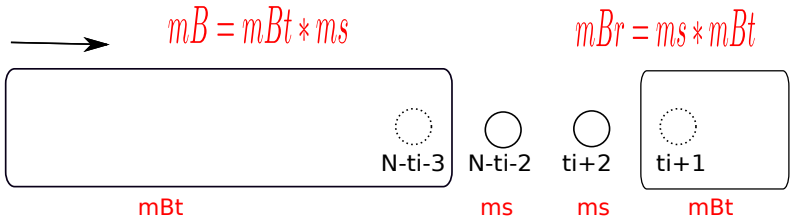

$$\text{size}(|\Psi_0\rangle) = mBt^2 * ms^2, 1$$

$$\tilde{\Psi} = reshape(|\Psi_0\rangle, mBr, mB)$$

$$\tilde{\Psi}_0 = \tilde{O}_L^{\dagger}\{N-ti-2\}\tilde{\Psi}(\mathbb{I} \otimes \tilde{O}_R\{ti+1\})^T$$

$$|\Psi\rangle = reshape(\tilde{\Psi}_0, mBr * mB, 1)$$

$$size(|\Psi\rangle) = mBt * ms^{ti+2}, 1$$

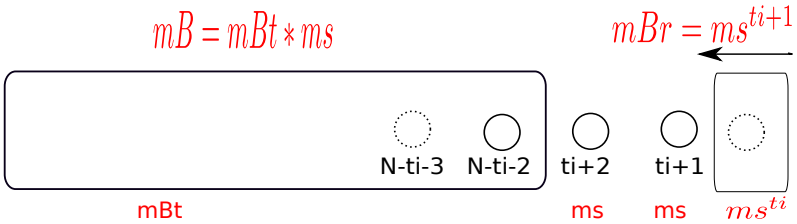

$$|\Psi\rangle_0 \approx |\Psi\rangle$$

$$\tilde{\Psi} = reshape(|\Psi_0\rangle, mBr, mB)$$

$$\tilde{\Psi}_0 = (\tilde{O}_L\{N-ti-2\} \otimes \mathbb{I})\tilde{\Psi}\tilde{O}_R\{ti+1\}$$

$$|\Psi\rangle = reshape(\tilde{\Psi}_0, mBr * mB, 1)$$

$$size(|\Psi\rangle) = mBt^2 * ms^2, 1$$

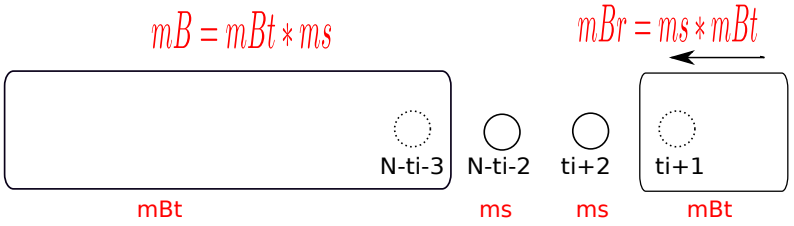

$$|\Psi\rangle_0 \approx |\Psi\rangle$$

Figure B.4: Wave function transformation formulas in the edge of the blocks where the direction of the sweep is changed. Wave function of a specific super-block configuration is used to predict the wave function of the next super-block configuration.

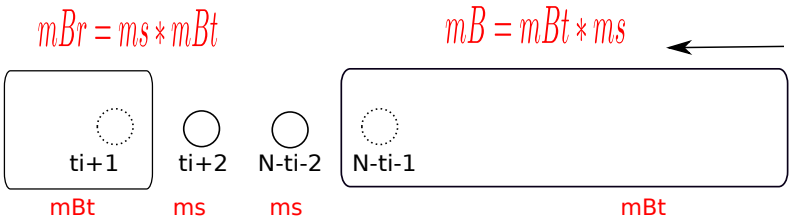

$$\text{size}(|\Psi_0\rangle) = mBt^2 * ms^2, 1$$

$$\tilde{\Psi} = reshape(|\Psi_0\rangle, mBr, mB)$$

$$\tilde{\Psi}_0 = (\tilde{O}_L\{ti+1\} \otimes \mathbb{I})\tilde{\Psi}\tilde{O}_R\{N-ti-2\}$$

$$|\Psi\rangle = reshape(\tilde{\Psi}_0, mBr * mB, 1)$$

$$size(|\Psi\rangle) = mBt * ms^{ti+2}, 1$$

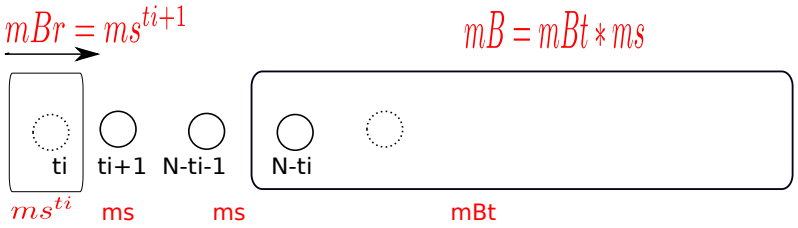

$$|\Psi\rangle_0 \approx |\Psi\rangle$$

$$\tilde{\Psi} = reshape(|\Psi_0\rangle, mBr, mB)$$

$$\tilde{\Psi}_0 = \tilde{O}_L\{ti\}\tilde{\Psi}(\mathbb{I} \otimes \tilde{O}_R\{N-ti-1\})$$

$$|\Psi\rangle = reshape(\tilde{\Psi}_0, mBr * mB, 1)$$

$$size(|\Psi\rangle) = mBt^2 * ms^2, 1$$

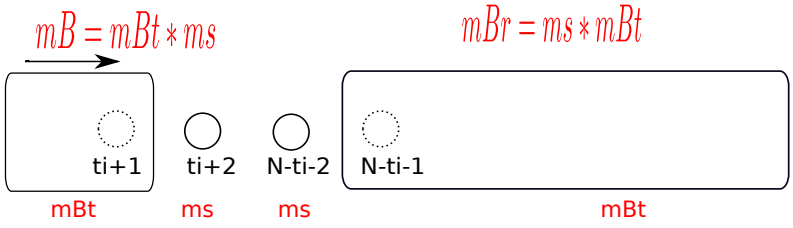

$$|\Psi\rangle_0 \approx |\Psi\rangle$$

Figure B.5: Wave function transformation formulas in the edge of the blocks where the direction of the sweep is changed.

Appendix C

Implemented Codes

C.1 Exact Diagonalization for the Dicke Model

main_dicke.m

```
Main program for the Dicke Model
```

```
clear all

N=2;
M=29;
J=1;
Omega=1;
V=1;
x0=10;
dt=1;

[basis0, d0] = FockStates(N,M);
[basis1, d1] = FockStates(N-1,M);

d=d0+d1;

Htb0=H_TB(basis0, d0, N, M, J);
Ha0=-Omega*eye(d0,d0);

Htb1=H_TB(basis1, d1, N-1, M, J);
Ha1=+Omega*eye(d1,d1);
```

```
Hint=H_int(basis0, basis1, d0, d1, N, M, x0, V);

H=[Htb0+Ha0 Hint; Hint' Htb1+Ha1];
[evec,eval]=eig(H);
psi=zeros(d,1);
psi((M+1)/2)=1;
U=expm(-1i*H*dt)';
for it=1:20
  psi=U*psi;
n_occ0=zeros(1,M);
for i=1:d0
  n=de2bi(basis0(i),M,N+1);
  n_occ0=n_occ0+abs(psi(i))^2*n;
end

n_occ1=zeros(1,M);
for i=d0+1:d0+d1
  n=de2bi(basis1(i-d0),M,N);
  n_occ1=n_occ1+abs(psi(i))^2*n;
end
dat0(1:M,it)=n_occ0;
dat1(1:M,it)=n_occ1;
end
```

FockStates.m

Formation of the Fock states for a given N, M

```
function [basis, d]=FockStates(N,M)

% M number of sites
% N number of photons

% number of balls + partitions

NT=N+M-1;
```

```
% dimension of the Hilbert space

d = nchoosek(NT,N);

% different positions of partitions
p=nchoosek(1:NT, M-1);

for i=1:d
    n(1)=p(i,1)-1;
    for j=2:M-1
       n(j)=p(i,j)-p(i,j-1)-1;
    end
    n(M)=NT-p(i,M-1);
    basis(i)=bi2de(n,N+1);
end
basis=sort(basis);
```

Tight Binding

Formation of Tight Binding Hamiltonian matrix

```
function HTB=H_TB(basis, d, N, M, J, U,  Vext)

HTB=zeros(d,d);
for i=1:d
n=de2bi(basis(i),M,N+1);
% diagonal on-site interaction
   HTB(i,i)=U/4*n(M)*(n(M)-1)+Vext(M)*n(M)/2;
for j=1:M-1
   HTB(i,i)=HTB(i,i)+U/4*n(j)*(n(j)-1)+Vext(j)*n(j)/2;
            if( n(j)>0 )
               k=find( basis == basis(i)-(N+1)^(j-1)+(N+1)^j );
      %look for the change in decimal when a j-1^th digit decreased
      %and j^th digit increased by 1
      HTB(i,k)=-J*sqrt( n(j)*(n(j+1)+1) );
   end
        end
% add periodic b.c.
% if( n(M)>0 )
% k=find( basis == basis(i)-(N+1)^(M-1)+1 );
```

```
% HTB(i,k)=sqrt( n(M)*(n(1)+1) );
% end
end
HTB=(HTB+HTB');
```

Interaction

Formation of interaction Hamiltonian matrix

```
function Hint=H_int(basis0, basis1, d0, d1, N, M, x0, V)

Hint=zeros(d0,d1);

for i=1:d1
     n=de2bi(basis1(i),M,(N-1)+1);
     n(x0)=n(x0)+1;
     k=bi2de(n,N+1);
     j=find( basis0 == k );
     Hint(j,i)=sqrt( n(x0)+1 );
end
Hint=V*Hint;
```

C.2 Tight Binding Model with tDMRG

Bibliography